

Silent calcium channels generate excessive tail currents and facilitation of calcium currents in rat skeletal myoballs

Andrea Fleig and Reinhold Penner

Department of Membrane Biophysics, Max-Planck-Institute for Biophysical Chemistry, Am Fassberg, 37077 Göttingen, Germany

1. Whole-cell patch-clamp recordings were employed to study facilitation of Ca^{2+} currents and excessive Ca^{2+} tail currents evoked by strong and long-lasting conditioning depolarizations in skeletal myoballs cultured from newborn rats.
2. Paired-pulse facilitation and excessive tail currents showed the same voltage dependence, becoming prominent at conditioning potentials above +30 mV.
3. Recruitment of excessive tail currents and facilitation occurred with the same time dependence (time constant (τ), ~200 ms to ~1 s), accelerating with the depolarization strength of conditioning pulses.
4. Reversal of Ca^{2+} current facilitation during the repolarization period between conditioning and test pulses was time- and voltage dependent. The time window of recruitment of facilitated Ca^{2+} currents narrowed considerably at more negative repolarization potentials (τ : ~10 ms at -100 mV, but ~1.5 s at 0 mV).
5. Neither omission of internal ATP nor perfusion of the cells with the peptide inhibitor of protein kinase A (PKI) had significant effects on Ca^{2+} current facilitation, although internal perfusion with ATP γ S slowly suppressed the facilitation currents by about 30%. External application of either ryanodine or caffeine under control conditions selectively and significantly suppressed the facilitated Ca^{2+} currents by about 30–40%.
6. We propose that facilitation of Ca^{2+} currents and excessive tail currents are consequences of a common mechanism linked to ryanodine receptors.

Calcium influx through voltage-dependent Ca^{2+} channels of electrically excitable cells is highly regulated by a multitude of mechanisms inducing up- or downregulation of N- and L-type channels. Some established modulatory mechanisms involve Ca^{2+} channel downregulation by G proteins (for review see Dolphin, 1990; Pelzer, Pelzer & McDonald, 1990; Porzig, 1990) or phosphorylation by protein kinase C (Scott & Dolphin, 1987) as well as Ca^{2+} channel upregulation by protein kinase A (Pelzer *et al.* 1990). Another common mechanism of Ca^{2+} channel modulation is provided by the membrane voltage itself (Fenwick, Marty & Neher, 1982; Hoshi, Rothlein & Smith, 1984; Artalejo, Dahmer, Perlman & Fox, 1991). This type of regulation manifests itself by an augmentation of Ca^{2+} currents following a conditioning prepulse to positive potentials and is often referred to as paired-pulse facilitation.

Paired-pulse facilitation of different degrees is observed for N-type as well as L-type Ca^{2+} channels and there may be distinct mechanisms responsible for Ca^{2+} channel facilitation in different cells (Fenwick *et al.* 1982; Hoshi *et al.* 1984; Elmslie, Zhou & Jones, 1990; Pietrobon & Hess, 1990; Artalejo, Rossie, Perlman & Fox, 1992; Sculptoreanu, Scheuer & Catterall, 1993). In the case of N-type Ca^{2+}

channels, it is believed that activated G proteins shift the activation curve of Ca^{2+} channels to more positive potentials, transferring them from a so-called 'willing' to a 'reluctant' state (Bean, 1989; Ikeda, 1991). Large and long-lasting depolarizations are thought to induce a voltage-dependent relief from the G protein inhibition, thereby recruiting reluctant channels into a willing state and facilitating their subsequent activation. Although the G protein regulation of N-type Ca^{2+} channels is well-established phenomenologically, its mechanism is not entirely understood.

The regulation of L-type Ca^{2+} channels appears to be even more complicated. For example, cardiac Ca^{2+} channels are upregulated by phosphorylation through cAMP-dependent protein kinase, even in the absence of a conditioning prepulse (Trautwein & Hescheler, 1990). In addition, strong depolarizations can induce a long-lived gating mode of L-type channels that is characterized by an increased open probability (Pietrobon & Hess, 1990). Voltage-dependent facilitation of Ca^{2+} currents in bovine adrenal chromaffin cells has been characterized in great detail by Fox and colleagues (Artalejo *et al.* 1991, 1992). Their data suggest that paired-pulse facilitation is mainly due to the

recruitment of normally quiescent L-type Ca^{2+} channels and is dependent on cAMP-dependent protein kinase. Similarly, Catterall and colleagues have proposed that paired-pulse facilitation in skeletal muscle requires both membrane depolarization and phosphorylation (Sculptoreanu *et al.* 1993; Johnson, Scheuer & Catterall, 1994). According to their hypothesis, strong and long-lasting depolarizations transfer L-type channels into a state in which they may be phosphorylated by protein kinase, resulting in facilitated Ca^{2+} currents during a subsequent depolarization. However, the facilitated current does not involve recruitment of quiescent L-type Ca^{2+} channels, but rather a shift of the activation of the channels to more negative potentials.

Our own studies of Ca^{2+} currents in skeletal muscle suggest the presence of at least two subsets of dihydropyridine-sensitive Ca^{2+} channels in skeletal muscle cells (Fleig & Penner, 1995): one subset with classical L-type channel characteristics and another with anomalous gating behaviour that is 'activated' or 'primed' by strong and long-lasting depolarizations without conducting significant Ca^{2+} current. However, upon repolarization, this subset of channels generates large tail currents. Interestingly, the voltage dependence and the kinetics of anomalous tail currents are similar to the activation of facilitation. We have therefore investigated the relationship between anomalous tail currents and facilitation in skeletal myoballs and provide evidence that facilitation is indeed accounted for by the recruitment of these tail currents. In our hands, facilitation appears to be primarily governed by membrane voltage with no apparent requirement of phosphorylation-dephosphorylation events.

METHODS

Rat skeletal myoballs were prepared from newborn rats (2–5 days old) essentially as described before (Fleig & Penner, 1995). For each preparation, one donor animal was anaesthetized with ether and decapitated. Colchicine treatment was omitted, as it appeared to render the cell membrane too fragile. Only rounded myoballs were used for whole-cell recordings. Patch-clamp experiments were performed in the tight-seal whole-cell configuration at 23–27 °C in an external solution containing (mM): NaCl, 140; KCl, 2.8; CaCl_2 , 10; MgCl_2 , 2; glucose, 11; TEA-Cl, 10; Hepes, 10; TTX, 0.005; pH 7.2 (equilibrated with HCl). Sylgard-coated patch pipettes had resistances of 1.5–3 M Ω after being filled with the standard intracellular solution which contained (mM): *N*-methyl-D-glucamine, 140; NaCl, 8; MgCl_2 , 1; Cs-EGTA, 20; Mg-ATP, 4; GTP, 0.3; Hepes, 10; pH 7.2 (equilibrated with HCl).

Membrane currents were acquired by a computer-based patch-clamp amplifier system (EPC-9; HEKA, Lambrecht, Germany). Capacitive currents were determined and compensated before each voltage pulse using the automatic capacitance neutralization of the EPC-9. Holding potential was usually –70 mV. Currents evoked during the depolarizing test pulses are referred to as 'pulse currents'. Currents evoked upon repolarization to more negative voltages than the test pulse are referred to as 'tail currents'. Pulse and tail current amplitudes are given as peak amplitudes or as charge. Series resistance compensation was not performed. Maximal voltage errors due to membrane capacitance (C_m) and

series resistance (R_s) were estimated to be about 9 mV at –70 mV with clamp speeds of around 105 μs (based on mean R_s values of 3.9 ± 0.2 M Ω , mean C_m values of 27 ± 2.4 pF ($n = 67$) and mean peak tail currents of 2.2 ± 0.37 nA ($n = 20$)). Currents were low-pass filtered at 8.8 kHz and digitized at 100 μs intervals (500 μs for data shown in Fig. 6). For analysis and presentation, currents were filtered digitally to 1–3 kHz.

The current–voltage (I – V) relationships of Ca^{2+} currents (I_{Ca}) were fitted with a Boltzmann function, a linear term, and a term for positive block to account for the non-linearity of the Ca^{2+} conductance above the reversal potential, according to:

$$I_{\text{Ca}} = g_{\text{max}}(V_m - E_{\text{rev}}) \times \frac{1}{1 + \exp(-[V_m - V_{1/2}]/\text{slope})} \times \frac{1}{1 + \exp(-[V_m - V_{1/2\text{block}}]/\text{slope}_{\text{block}})}, \quad (1)$$

where g_{max} is the maximal conductance, V_m is the test potential, E_{rev} is the reversal potential and $V_{1/2}$ is the voltage at half-maximal activation. The theoretical activation curve of tail currents was determined by first fitting the I – V curve plotted in Fig. 2C. The resulting values of $V_{1/2}$ and the slope factor (see Fig. 1B) were kept fixed and fitted to the activation curve of the tail current (I_{tail}) in the range –50 to +10 mV according to:

$$I_{\text{tail}} = I_{\text{max}} \times \frac{1}{1 + \exp(-[V_m - V_{1/2}]/\text{slope})}, \quad (2)$$

to obtain an estimate of the maximum current (I_{max}). Activation and deactivation kinetics were approximated by mono- or biexponential fits. The degree of facilitation was estimated from current integrals. Throughout, data are given as means \pm s.e.m. with n determinations and, where appropriate, statistical analysis was performed by applying Student's t test.

RESULTS

Facilitation of Ca^{2+} currents

Calcium currents in rat skeletal myoballs were recorded in 10 mM $[\text{Ca}^{2+}]_o$, with Na^+ channels blocked by 5 μM TTX and K^+ currents inhibited by extracellular TEA (10 mM) and by using *N*-methyl-D-glucamine (140 mM) to replace K^+ as the intracellular monovalent cation. Figure 1A illustrates a typical example of Ca^{2+} current facilitation by comparing superimposed control and facilitated current records. Control currents of 300 ms duration were recorded in response to depolarizing voltage pulses to different potentials, while the corresponding facilitation currents were preceded by a conditioning pulse to +80 mV for 600 ms and a brief return to the resting potential for 20 ms. The conditioning pulse induced a marked augmentation of the subsequent pulse currents at test potentials in the range –20 to +10 mV (Fig. 1A). From the average I – V relationships of control and facilitated Ca^{2+} currents ($n = 5$), it can be seen that the voltage dependence of facilitated Ca^{2+} currents was shifted by about 10 mV to the left compared with the control currents ($P < 0.01$; Fig. 1B). Since Ca^{2+} currents at more positive potentials are not potentiated, it appears that facilitation is not due to a change in open probability of Ca^{2+} channels, but rather to a change in the voltage dependence of the same channels that produce the

control currents or to the recruitment of an additional population of previously 'silent' Ca^{2+} channels.

Voltage dependence of facilitation

Facilitation of Ca^{2+} currents requires strong prepulse depolarizations. To assess the voltage dependence of facilitation, the conditioning prepulse of 600 ms was stepped to different voltages and was followed by a brief return to the holding potential for 20 ms. The subsequent test pulse to 0 mV revealed potentiated Ca^{2+} currents depending on the prepulse voltage. A typical example of this voltage-dependent potentiation is illustrated in Fig. 2A. The average voltage dependence of facilitation ($n = 5$) was measured by normalizing the total charge of the potentiated currents for the unconditioned control currents and was plotted as a function of the prepulse potential (Fig. 2B). It can be seen that prepulses below +30 mV caused a minor reduction of the test pulse, possibly due to Ca^{2+} -dependent inactivation, whereas stronger depolarization progressively increased the degree of facilitation.

We have previously reported the presence of a population of Ca^{2+} channels with 'anomalous' gating behaviour in skeletal muscle (Fleig & Penner, 1995). These channels do not carry significant current during depolarizations, but generate large tail currents upon repolarization to negative potentials. The voltage dependence of these 'anomalous' tail currents is strikingly similar to the voltage dependence of facilitation. To illustrate this similarity, we assessed the voltage dependence of pulse currents and tail currents evoked by the conditioning prepulse. Figure 2C shows plots of the average I - V relationship of pulse currents (measured during the last 10% of each conditioning pulse; $n = 5$) and the peak amplitude of tail currents following repolarization to -70 mV.

The plot of the pulse currents reveals the typical behaviour of high-voltage-activated Ca^{2+} channels with inward currents activating at about -30 mV and peaking around +10 mV. The tail currents activate in parallel with the pulse currents but there seems to be a further increase at very

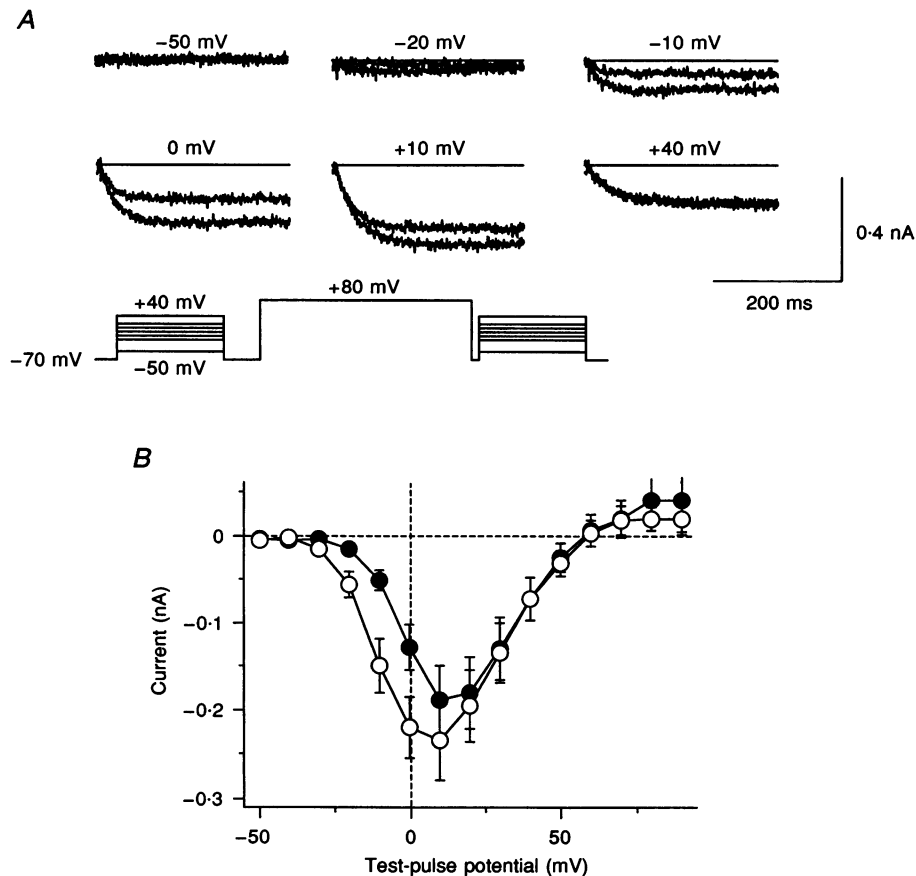


Figure 1. Strong depolarizations induce facilitation

A, Ca^{2+} currents evoked by a double-pulse protocol with a prepulse length of 600 ms. Prepulse-conditioned Ca^{2+} currents were measured at variable test-pulse potentials for 300 ms following a 20 ms repolarization to holding potential (-70 mV). Each prepulse was preceded by a 300 ms control pulse. The delay between control and prepulse was 100 ms. Depicted are test potentials between -50 and +40 mV. B, I - V curves of control (●; $V_{1/2} = 7 \pm 2$ mV; slope = 7 ± 0.2 mV; $g_{\max} = 8.8 \pm 2.4$ nS; $E_{\text{rev}} = 62 \pm 7$ mV; $n = 5$) and conditioned test pulses (○; $V_{1/2} = -8 \pm 4$ mV; slope = 7 ± 1 mV; $g_{\max} = 7.3 \pm 1.6$ nS; $E_{\text{rev}} = 61 \pm 7$ mV; $n = 5$; statistical relevance for $V_{1/2}$: $P < 0.01$). The I - V fit was done using eqn (1). Protocol as described in A.

depolarized potentials. We determined the theoretical activation curve of Ca^{2+} currents by fitting the $I-V$ relationship to eqn (1) and using its $V_{1/2}$ and slope values as fixed parameters in a Boltzmann function (eqn (2), see Methods). The fitted Boltzmann term is plotted as a dashed line in Fig. 2C and reflects the theoretical size of the tail currents expected to be generated by the preceding pulse currents. However, there is a clear deviation of the theoretical tail currents from the measured ones. This difference reflects the contribution of additionally recruited anomalous tail currents and is plotted as the difference current in Fig. 2D. It can be seen that the anomalous tail currents have a similar voltage dependence as the facilitation currents (Fig. 2B), since both grew in parallel.

Time dependence of facilitation

Facilitation of Ca^{2+} currents requires long-lasting prepulse depolarizations. To assess the time dependence of facilitation, the conditioning prepulses were stepped to different voltages

for variable periods of time and were followed by a brief return to the holding potential for 20 ms. The subsequent test pulses to 0 mV revealed potentiated Ca^{2+} currents depending on the prepulse voltage and duration. Typical examples of this voltage- and time-dependent potentiation are illustrated in Fig. 3A. The amount of facilitation was quantified by normalizing the total charge of the potentiated currents for the unconditioned control currents and was plotted as a function of the prepulse duration (Fig. 3B; $n = 4$). Obviously, facilitation increases with stronger depolarizations and longer prepulse durations. Saturation of this effect occurs at voltages around +100 mV and prepulse durations of 2–3 s.

We have previously reported that tail currents exhibit two exponential components, a fast component that matches the activation time course of the pulse currents (~ 40 ms) and a slower component that is due to the recruitment of anomalous tail currents (~ 150 to ~ 600 ms, depending on

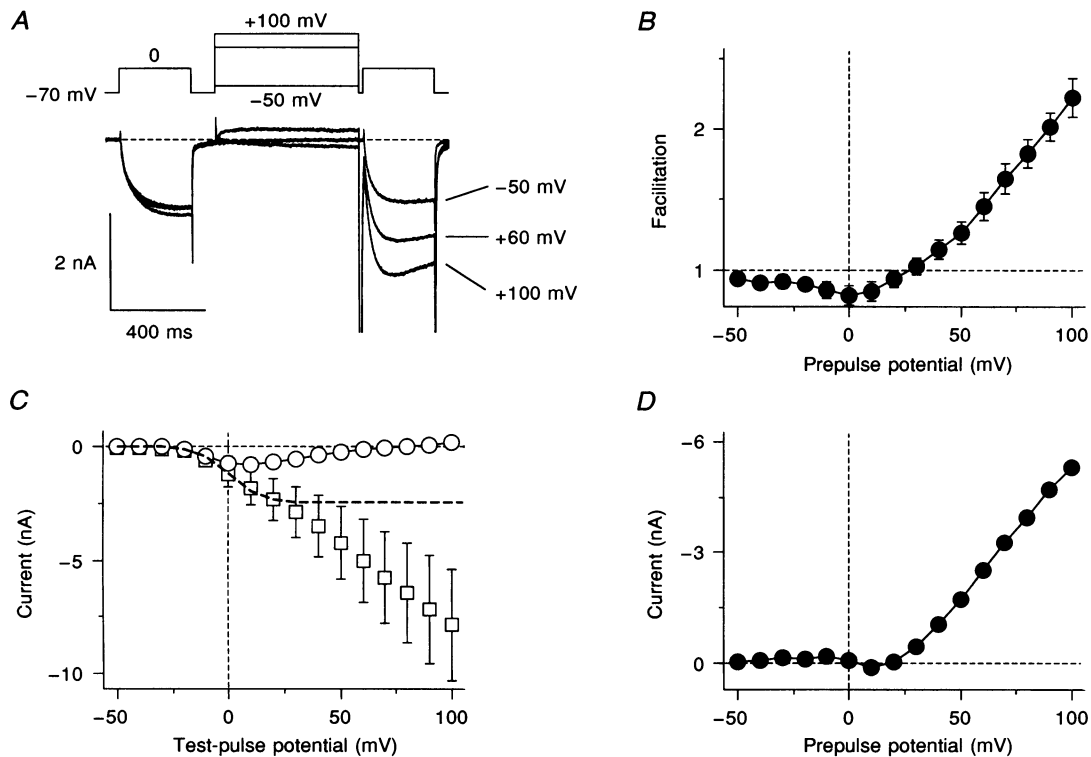


Figure 2. Voltage dependence of facilitation

A, Ca^{2+} currents evoked by a double-pulse protocol which varied the prepulse potential to -50, +60 and +100 mV. Prepulse-conditioned Ca^{2+} currents were measured at 0 mV for 300 ms following a 20 ms repolarization to holding potential (-70 mV). Prepulse length was 600 ms. Each prepulse was preceded by a 300 ms control pulse to 0 mV. The delay between control and prepulse was 100 ms. B, voltage dependence of facilitation evoked by prepulses of 600 ms to variable potentials ($n = 5$). Pulse protocol was as described in A. The total charge of both control and prepulse-conditioned test pulses was measured and each conditioned pulse was then normalized to its respective control pulse and plotted *versus* prepulse potential. C, $I-V$ curve (○) and activation curve (□), plotted *versus* test-pulse potential ($n = 5$). Depolarization length was 600 ms. The dashed line represents the theoretical activation curve as modelled by eqn (2) (parameters were taken from the fit to the $I-V$ curve (see Fig. 1B) with $I_{\text{max}} = -2.47$ nA). D, the difference current of the theoretical activation curve and the actual activation curve as shown in C.

the voltage). Again, the time course of facilitation is strikingly similar to the kinetics of the recruitment of 'anomalous' tail currents. To illustrate this similarity, we assessed the time dependence of tail currents evoked by the conditioning prepulse. Figure 3C shows plots of the normalized mean peak amplitude of tail currents following repolarization to -70 mV. It can be seen that the anomalous tail currents had a similar time dependence as the facilitation currents, since both grew and saturated in

parallel. Figure 3D illustrates the kinetic analysis of these data as assessed by exponential fits to the time course of the development of facilitation and tail currents obtained at different prepulse depolarizations. The time course of facilitation was fitted by a single exponential function, whereas tail currents required the sum of two exponentials (only the slower component is plotted in Fig. 3D; n = 4). The fast component had time constants around 40 ms.

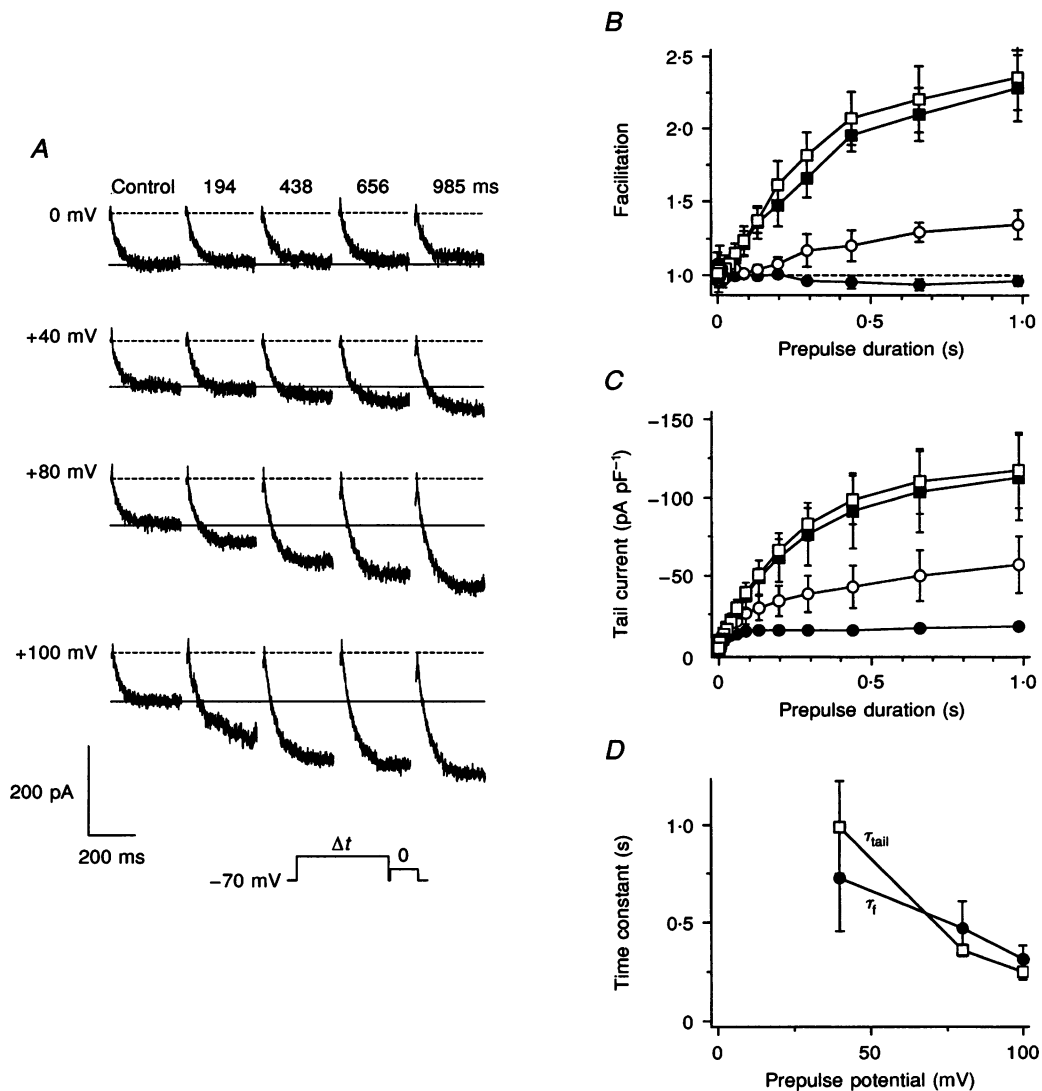


Figure 3. Time dependence of facilitation

A, Ca²⁺ currents evoked by a double-pulse protocol with a fixed prepulse potential to either 0, +40, +80 or +100 mV and increasing depolarization durations (Δt). Prepulse-conditioned Ca²⁺ currents were measured for 300 ms at 0 mV following a 20 ms repolarization to holding potential (-70 mV). All traces are from the same cell. B, degree of facilitation plotted versus the respective prepulse duration. Same protocol as in A. Facilitation was calculated by dividing the total charge of the conditioned test pulses by the charge of the control pulse. Prepulse potentials of 0 (●), +40 (○), +80 (■) and +100 mV (□) are shown (n = 5 for +80 mV; n = 4 for the other potentials). C, tail current peak amplitudes (normalized to cell capacitance) evoked by variable test-pulse lengths to distinct test-pulse potentials (0 (●), +40 (○), +80 (■), +100 mV (□)) and repolarization to holding potential (-70 mV) and plotted as a function of the prepulse duration. Same n values as in B. D, voltage dependence of the activation time constants for anomalous gated tail currents (τ_{tail} , □; n = 4) and facilitation (τ_f , ●; same n values as in B).

Dependence of facilitation on repolarization voltage

In a further series of experiments, we investigated the effects of repolarization on facilitation. The conditioning prepulse of 600 ms was stepped to +80 mV and was followed by a brief return to variable repolarization potentials for 20 s. The subsequent test pulse to 0 mV revealed potentiated Ca^{2+} currents depending on the repolarization voltage. Typical examples of this repolarization-dependent potentiation are superimposed in Fig. 4A and compared with the control current (inset in Fig. 4A). The dependence

of facilitation on the repolarization voltage ($n = 4$) was measured by integrating the control and potentiated currents over 160 ms and calculating their ratio. This analysis yields the amount of facilitation and is plotted as a function of the repolarization potential in Fig. 4B. It can be seen that repolarization to positive voltages produced the largest facilitation, whereas stronger hyperpolarizations progressively decreased the amount of facilitation. At the same time, there was also a progressive increase in the rate of deactivation of tail currents at more negative potentials.

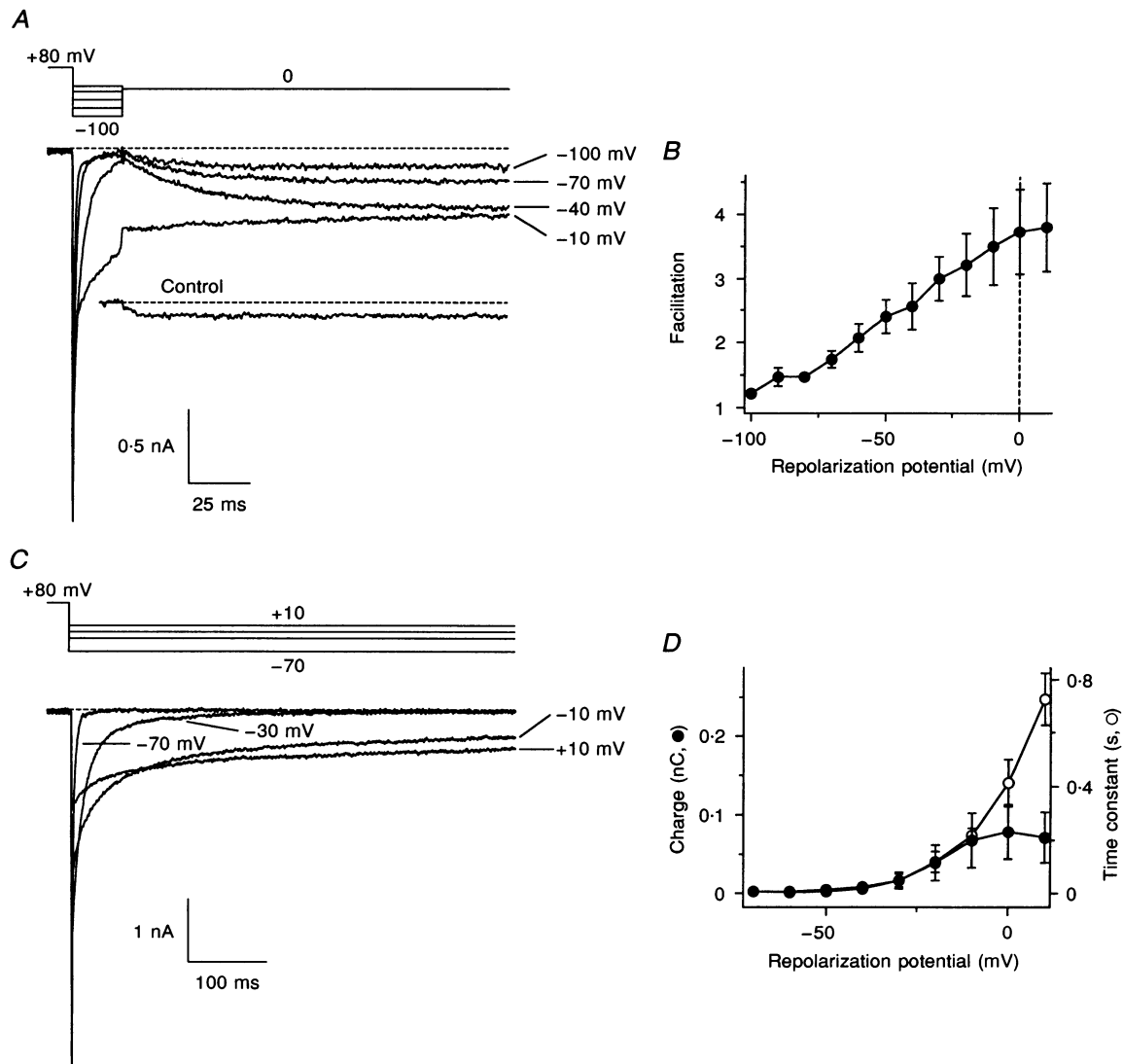


Figure 4. Dependence of facilitation on repolarization potential

A, traces with repolarization of 20 ms and -100 to -10 mV followed by a test pulse to 0 mV and 300 ms length. Conditioning pulses were 600 ms to +80 mV. Each prepulse was preceded by a 300 ms control pulse to 0 mV. The delay between control and prepulse was 100 ms. *B*, total charge of the prepulse-conditioned test pulse to 0 mV and 160 ms divided by the charge of the control current plotted *versus* repolarization potential ($n = 4$). The mean charge of the control currents was 18 ± 0.2 pC ($n = 4$). Conditioning pulses were 600 ms to +80 mV. Repolarization length was 20 ms. *C*, data traces of four different repolarization potentials following a conditioning pulse of 600 ms to +80 mV. *D*, voltage dependence of the slow deactivation time constants (○; $n = 4$) and amount of charge (●; $n = 4$) as a function of the repolarization potential. Total charge measured over 160 ms repolarization duration, starting 20 ms after the onset of repolarization.

As is evident from the current records in Fig. 4A, the time course of the decay of tail currents is slow at positive potentials but becomes progressively faster at more negative repolarizing potentials. Figure 4C illustrates the decay of tail currents evoked by a similar voltage protocol as in Fig. 4A but without a facilitation test pulse. In general, the decay of tail currents followed a biexponential time course. We have previously shown that the fast deactivation is probably due to the tail currents associated with 'normal' Ca²⁺ channels that carry the pulse currents, whereas the slow component is attributable to the recruitment of anomalous tail currents. At more positive repolarizations, this slow component decays with time constants of several hundreds of milliseconds and represents the major current component of the total tail current (see records at +10 or -10 mV in

Fig. 4C). More negative repolarizations (e.g. -30 mV) increase the rate of decay of this slow component until at very negative repolarizations, the slow and fast components of tail current deactivation merge and produce an almost monoexponential decay. Figure 4D shows plots of both the deactivation time constants of the slow tail current component as a function of repolarization potential and the current integral measured over 160 ms (starting 20 ms after the onset of repolarization). Clearly, with slower deactivation of tail currents, there is substantially more current flowing during the repolarization and the current integral increases in parallel with the slowing of deactivation. The divergence of the two curves at positive potentials reflects the decrease in driving force for Ca²⁺ influx at more positive potentials, causing the current integral to level off.

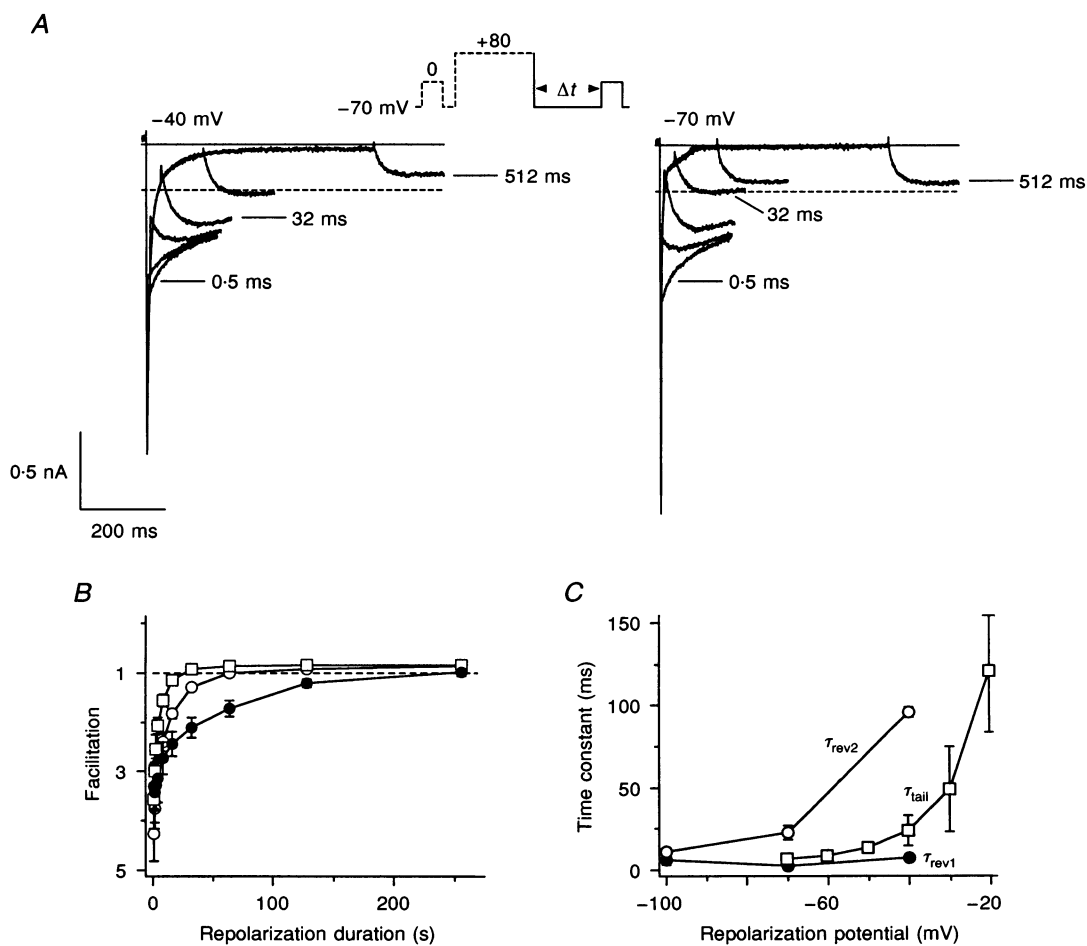


Figure 5. Reversal of facilitation

A, reversal of facilitation by incrementing interpulse durations between conditioning and test pulse (Δt). Depicted are repolarization potentials to -40 mV (left panel) and -70 mV (right panel). Conditioning pulses were 600 ms to +80 mV. Each prepulse was preceded by a 160 ms control pulse to 0 mV. The delay between control and prepulse was 100 ms. Data are from the same cell. B, total charge of the prepulse-conditioned test pulse to 0 mV and 160 ms divided by the charge of the control-pulse current and plotted versus repolarization duration. The dependence of the reversal of facilitation on the repolarization potential is given for -40 (●; n = 4), -70 (○; n = 6) and -100 mV (□; n = 4). C, voltage dependence of time constants for slow deactivation (τ_{tail} , □; n = 4) and reversal of facilitation (τ_{rev1} , ●; τ_{rev2} , ○; same n values as in B). Protocol for reversal of facilitation as described in A.

Dependence of facilitation on repolarization duration

For facilitation to occur, the test pulse needs to be delivered within short periods of time following the conditioning pulse. Increasing the repolarization phase between conditioning and test pulse by prolonging the interpulse interval will gradually revert the facilitation of the subsequent test pulse. This 'reversal' of facilitation is also voltage dependent and proceeds faster at more negative repolarization potentials of the interpulse. Figure 5A illustrates this phenomenon for two repolarization potentials (-40 and -70 mV). The superimposed current records display the amount of facilitation of a test pulse to 0 mV obtained following a variable repolarization phase. The dashed lines indicate the current amplitudes of the control pulse delivered before the conditioning pulse. It can be seen that the Ca^{2+} current was still potentiated about twofold after 32 ms of repolarization to -40 mV, whereas at

-70 mV the same interpulse duration failed to produce significant facilitation. Longer interpulse durations were typically followed by test-pulse currents that were even slightly smaller than the control currents, possibly due to a small Ca^{2+} -dependent inactivation of the currents.

The mean reversal of facilitation for three different repolarization potentials as a function of the interpulse duration is shown in Fig. 5B ($n = 6$ for -70 mV; $n = 4$ for -40 and -100 mV). The time course of this reversal was characterized by a fast and a slow component. The fast component was relatively voltage independent and had a time constant of ~ 10 ms. The second component was considerably slower at less negative potentials (e.g. -70 or -40 mV). The two time constants resulting from a biexponential fit to these data are plotted in Fig. 5C as τ_{rev1} and τ_{rev2} (same n values as in Fig. 5B). When the reversal of facilitation is compared with the slow deactivation of tail

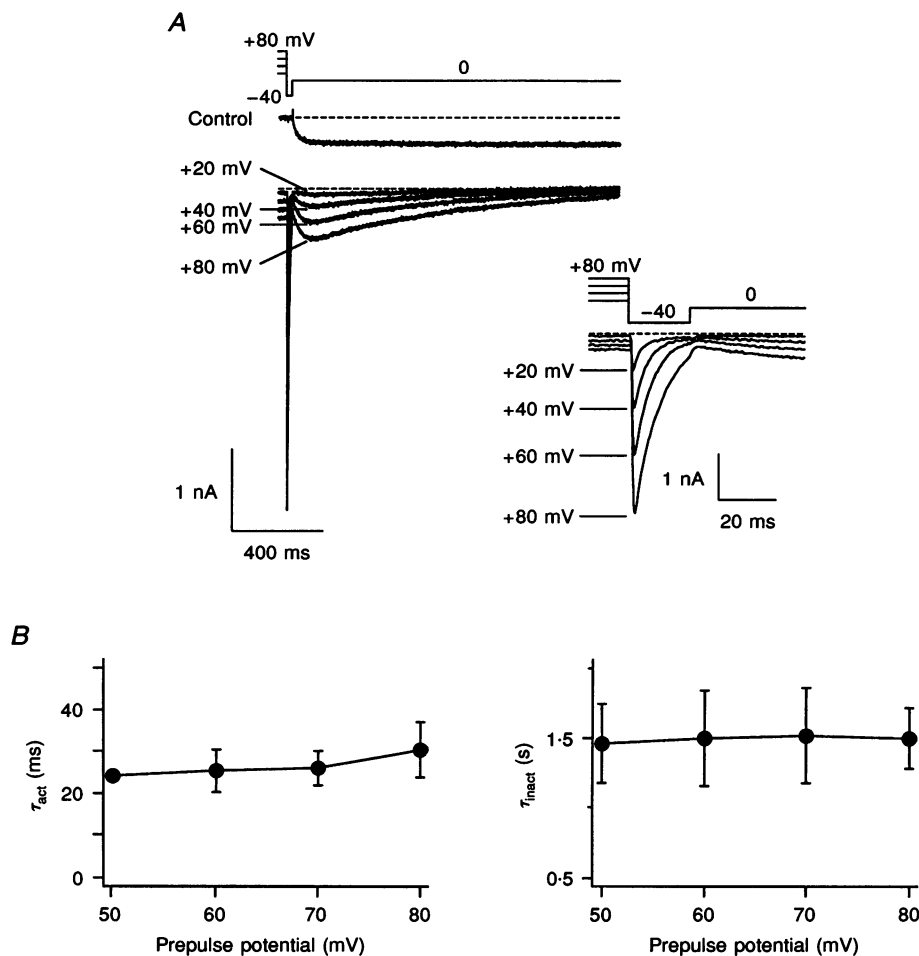


Figure 6. Activation and inactivation of facilitation currents

A, average raw data of control currents and the net facilitation current obtained by subtracting the control current from the facilitated current ($n = 5$). Conditioning pulses were 600 ms to $+20$, $+40$, $+60$ and $+80$ mV. Repolarization was 20 ms to -40 mV. Each prepulse was preceded by a 1.5 s control pulse to 0 mV. The delay between control and prepulse was 100 ms. The inset shows the same data at a higher temporal resolution. B: left panel, mean activation time constants (τ_{act}) of the net facilitation current plotted versus the prepulse potential ($n = 3$ each point); right panel, mean inactivation time constants (τ_{inact}) of the net facilitation current plotted versus the prepulse potential ($n = 3$ each point).

currents (τ_{tail} in Fig. 5C; $n = 4$), it is evident that the reversal of facilitation does not match exactly the decay of the anomalous tail currents. Rather, facilitation can persist longer than the actual deactivation of the tail currents and it is therefore unlikely that the facilitation is simply the carry-over of the deactivating tail currents superimposing on the pulse currents evoked by the test pulse.

Activation and inactivation of facilitation currents

Previous work on facilitation of skeletal muscle suggested that the depolarization during the conditioning pulse shifted the voltage dependence of the 'normal' Ca^{2+} channels to the left, such that a subsequent test pulse to the same potential as the control pulse would activate more channels and appear facilitated (Sculptoreanu *et al.* 1993). If this were the only effect of the conditioning depolarization, one would expect the facilitated Ca^{2+} currents to behave essentially like the unfacilitated pulse current, except that they would display a larger amplitude and perhaps faster activation kinetics. On the other hand, the experiments described here suggest that facilitation occurs in parallel with the recruitment of anomalous tail currents rather than a change in open probability or voltage dependence of the 'normal' Ca^{2+} channels activated during a control pulse. Since voltage dependence and kinetics of anomalous tail currents are strikingly different from the 'normal' pulse currents, we wondered if the additional current component recruited by a conditioning pulse (the 'net' facilitation current) might reveal properties that are different from the behaviour of the normal pulse currents.

We assessed the properties of the net facilitation current by subtracting the control current from the facilitated current (Fig. 6A; $n = 5$). The difference between the two is the net current that is recruited by the conditioning pulse. The inset to Fig. 6A shows a higher temporal resolution of the same data to illustrate more clearly the increase in tail current associated with stronger depolarizations during the conditioning pulse. From these data it is clear that stronger depolarizations recruit both larger tail currents and more facilitation. The net facilitation current, however, has distinct features that set it apart from the behaviour of the control-pulse current. Most notably, net facilitated currents inactivate completely with a time constant of about 1.5 s at 0 mV ($n = 3$). The activation kinetics of control and facilitated currents were similar (19.3 ± 2.5 and 24 ± 1 ms at 0 mV, respectively; $n = 3$ each). These parameters, which show little voltage dependence, are plotted as a function of the conditioning prepulse in Fig. 6B.

Modulation of facilitation

It has been suggested that the mechanism of facilitation in skeletal muscle involves voltage-dependent phosphorylation of Ca^{2+} channels by cAMP-dependent protein kinase (Sculptoreanu *et al.* 1993; Johnson *et al.* 1994). This interpretation is based on experiments in which omission of ATP from the pipette filling solution or inclusion of the peptide inhibitor of protein kinase A (PKI) blocked

facilitation almost completely. We have reinvestigated the effects of PKI, ATP withdrawal, and ATP γ S on facilitation by monitoring the degree of facilitation over a time period of 15 min after establishment of the whole-cell configuration. At regular intervals of 20 s, we applied a 300 ms control pulse to 0 mV, followed by a conditioning pulse of 600 ms to +80 mV, a 20 ms repolarization to -40 mV, and finally a 300 ms test pulse to 0 mV. The amount of facilitation in a given cell was assessed by measuring the current integral of the test and control pulse and calculating the ratio. After 100 s of whole-cell recording (5th stimulus protocol), which is the time required to replace the internal K^+ by Cs^+ and establish stable recording conditions, we calculated the degree of facilitation using the value of the 5th stimulus protocol to normalize the degree of facilitation of all subsequent stimuli. The effects of the various pharmacological interventions are illustrated in Fig. 7A.

When the standard internal solution (which contained 4 mM ATP) was used, facilitation was very stable and well maintained over 15 min of recording ($n = 7$). In contrast to a previous study (Sculptoreanu *et al.* 1993), there was no significant effect on facilitation when ATP was omitted from the internal solution ($n = 6$). Furthermore, there was only a small reduction in the degree of facilitation of 10–20% when the internal solution was supplemented with 10 μM PKI ($n = 8$). Even more surprisingly, when cells were perfused with internal solutions in which the ATP was replaced by 1 mM ATP γ S, an ATP analogue that is readily used by kinases for phosphorylation, there was an even greater decrease in facilitation ($n = 5$). We found no obvious effect of ATP γ S on either the deactivation of tail currents or the activation kinetics of facilitation. Furthermore, there was no change in the rate of activation or inactivation of the net facilitation current (data not shown). Essentially identical results were obtained when 100 μM ATP γ S added to the standard internal solution (which contained 4 mM ATP) was used. Together, these data do not support the notion that phosphorylation is an essential mechanism for facilitation, but that it appears to modulate it by an unknown mechanism.

We tested ryanodine and caffeine for possible effects on facilitation, based on the idea that anomalous tail currents are silent Ca^{2+} channels that are somehow blocked (possibly by the interaction with ryanodine receptors (RyRs) during excitation–contraction (E–C) coupling) and conduct when this block is alleviated to produce facilitation (see Discussion). Indeed, external application of ryanodine (100 nM) or caffeine (10 mM), which both interact with RyRs, consistently reduced facilitation currents. The average reduction of facilitation induced by ryanodine was $28 \pm 5\%$ ($n = 5$; $P < 0.05$) and caffeine inhibition was $35 \pm 4\%$ ($n = 9$; $P < 0.05$; Fig. 7B). At the same time, the peak tail currents following the conditioning pulse were reduced by 21 ± 5 and $30 \pm 4\%$, respectively. The effect of both caffeine (Fig. 7C) and ryanodine (raw data not shown) was selective for facilitation currents, since control currents

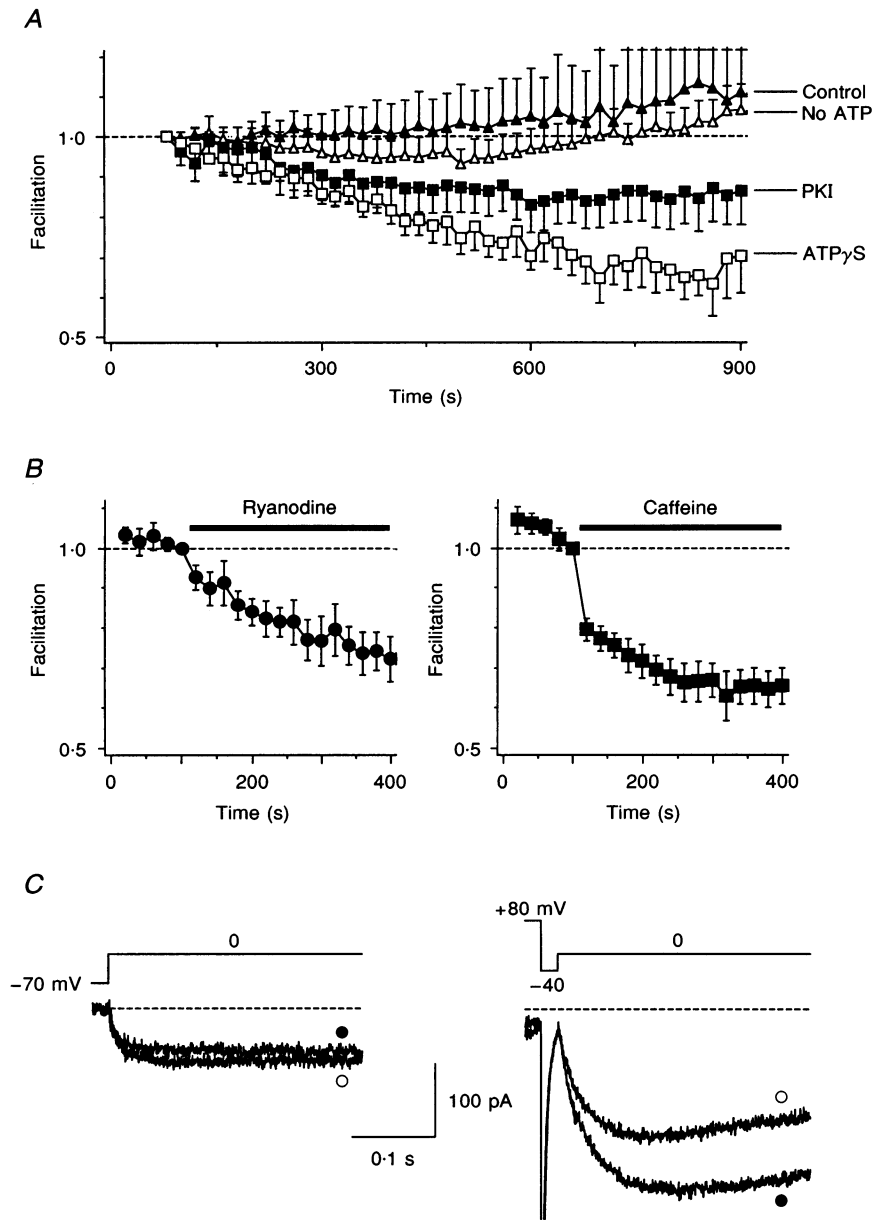


Figure 7. Modulation of facilitation

A, mean degree of facilitation under control conditions (\blacktriangle ; $n = 7$), omission of ATP (\triangle ; $n = 6$), addition of $10 \mu\text{M}$ PKI (\blacksquare ; $n = 8$) and 1 mM ATP γ S (\square ; $n = 5$) plotted *versus* whole-cell perfusion time. The stimulus protocol was a 300 ms control pulse to 0 mV, followed by a conditioning prepulse of 600 ms to +80 mV and a test pulse to 0 mV after a repolarization of 20 ms to -40 mV. The delay between control and prepulse was 100 ms. The degree of facilitation per cell was calculated by integrating control and test pulses and calculating their ratio. The 5th stimulus protocol (100 ms whole-cell time) was used to normalize the degree of facilitation of the following stimuli. Stimulus intervals were 20 s. *B*, application of 100 nM ryanodine (\bullet , left panel; $n = 5$) or 10 mM caffeine (\blacksquare , right panel; $n = 9$). The period of application is indicated by the filled bars. Same stimulus protocol and calculation of degree of facilitation as in *A*, except that stimulus protocols were started 1 min after whole-cell formation. Application began after the 5th stimulus, which was also used as control. *C*, typical raw data traces of an example cell before (\bullet) and after (\circ) 5 min of 10 mM caffeine application. Left panel, control pulses; right panel, facilitated currents. Same stimulus protocol as in *A*.

were essentially unaffected. This seems to suggest that the RyR might interact with the Ca^{2+} channels in the plasma membrane to modify their behaviour, but that this interaction is restricted to the phenomenon of facilitation and does not affect the normal Ca^{2+} currents.

DISCUSSION

Facilitation of Ca^{2+} currents in rat skeletal myoballs manifests itself as a large increase in current amplitude following conditioning depolarizations to positive voltages for prolonged periods of time. The $I-V$ relationship of facilitated currents reveals that there is an apparent shift in the activation curve of facilitated Ca^{2+} currents to more negative potentials compared with control currents without conditioning prepulses (see Fig. 1). This shift is only about 10 mV, but it will effectively augment Ca^{2+} currents at moderate depolarizations, because more channels conduct at potentials at which the driving force for Ca^{2+} is larger. Facilitation does not seem to be due to a change in the open probability of the Ca^{2+} channels, since Ca^{2+} currents at potentials above +20 mV are not facilitated.

Previous work has indicated that Ca^{2+} currents can be modulated by preceding depolarizations. In cut muscle fibres of the frog, a kinetic mode switch occurs between the normal slow mode of L-type Ca^{2+} channel gating and a fast activation mode (Feldmeyer, Melzer, Pohl & Zöllner, 1990, 1992). This switch from slow to fast mode is induced by conditioning prepulses to voltages around the threshold of channel activation (~ -40 mV) and is not accompanied by facilitation of Ca^{2+} currents. The authors concluded that the switch is closely connected to a conformational transition of the channel from the closed to the open state. In rat skeletal myoballs, we have not observed a striking effect of prepulse depolarizations on the kinetic behaviour of the pulse currents. Instead, we found a strong potentiation of Ca^{2+} currents following strong and long-lasting depolarizations, which is in good agreement with the original observations made by Catterall and co-workers (Sculptoreanu *et al.* 1993; Johnson *et al.* 1994). These latter studies, also carried out in rat skeletal myoballs, suggested phosphorylation of L-type channels as the mechanism of facilitation. According to this hypothesis, strong and long-lasting depolarizations induce a voltage-dependent phosphorylation of Ca^{2+} channels by somehow exposing phosphorylation sites to cAMP-dependent protein kinase. The phosphorylation then causes a transient shift in the activation curve of the channels to more negative potentials, such that a subsequent test pulse exhibits potentiated currents. This effect is transient and reversed by dephosphorylation by an okadaic acid-sensitive protein phosphatase, possibly phosphatase 1 or 2A.

Some of our present data are in contrast to these latter studies. For example, we did not observe a striking dependence of facilitation on the presence of intracellular ATP, as the inclusion or omission of 4 mM ATP in the patch pipette did not affect the amount of facilitation (see Fig. 7).

Neither did PKI, previously reported to block facilitation by about 75% (Sculptoreanu *et al.* 1993), substantially compromise facilitation under our experimental conditions, although it did cause a small decrease in facilitation of about 10–20%. We have no obvious explanation for these discrepancies. In a further set of experiments using ATP γ S, we also failed to establish a correlation between phosphorylation and facilitation. With ATP γ S, an ATP analogue that is readily used by kinases to irreversibly phosphorylate target proteins, one would have expected a persistent phosphorylation of Ca^{2+} channels which cannot be removed by phosphatases. As a consequence, one might have predicted an upregulation of control currents as phosphorylated channels should remain permanently in the facilitated state. Instead, we observed a reduction in facilitation (about 30%) in the absence of an increase in normal Ca^{2+} currents.

There are some further points that make it difficult to accommodate our data in a scheme that involves phosphorylation and dephosphorylation. The first point concerns the reversal of facilitation, which is clearly voltage dependent and can occur with a time constant of about 10 ms when repolarizing to -100 mV (see Fig. 5). According to the phosphorylation–dephosphorylation hypothesis, this reversal reflects the rate of dephosphorylation and one would be forced to conclude that the rate of dephosphorylation not only exceeds the rate of phosphorylation (which is the time constant of the recruitment of facilitation; see Fig. 3), but also is faster than the opening of the Ca^{2+} channels themselves (which is about 40–50 ms). Furthermore, in our experiments the reversal of facilitation was completely unaffected by ATP γ S (see Results). A second point concerns the activation curve of Ca^{2+} channels as reflected by the voltage dependence of tail currents. If phosphorylation simply shifted the activation curve of 'normal' Ca^{2+} channels to the left, then we would expect the tail currents to reflect this shift. However, the opposite is true: long-lasting and strong depolarizations recruit larger and larger tail currents at more positive potentials (this point will be discussed later). A third point relates to the selective suppression of facilitation by caffeine and ryanodine, which is not likely to involve phosphorylation or dephosphorylation events. In summary, our data on Ca^{2+} current facilitation are not easily accounted for by phosphorylation–dephosphorylation. Instead, we favour an alternative explanation based on the voltage- and time-dependent recruitment of 'silent' Ca^{2+} channels.

In a recent study, we demonstrated the presence of excessive tail currents in skeletal muscle, which were activated by strong and long-lasting depolarizations (Fleig & Penner, 1995). These tail currents are due to the anomalous gating of a subset of dihydropyridine-sensitive Ca^{2+} channels that do not carry significant current during depolarization ('silent' channels) but conduct upon repolarization. The excessive tail currents upon repolarization are as instantaneous as we can measure (essentially limited by

clamp speed, which is about 100 μ s). Thus we most probably do not have a transition between different states of the Ca^{2+} channels themselves (the Ca^{2+} channels are in the open state during the depolarization) (Pietrobon & Hess, 1990). We have previously suggested that a possible reason for the absence of current flow through these channels during the depolarization is due to a 'blocking particle' of unknown nature (tentatively the RyR). The presence of such silent Ca^{2+} channels constitutes a potential source for facilitation, especially since the present study establishes a striking correlation between the recruitment of anomalous tail currents and the manifestation of facilitation following strong and long-lasting prepulse depolarizations. Both voltage- and time dependence of anomalous tail currents and the degree of facilitation are essentially identical (see Figs 2 and 3), indicating that both processes might be interrelated. In the following section and Fig. 8, we would like to propose a hypothetical model which could account for facilitation as a result of the recruitment of 'silent' channels.

There are two populations of dihydropyridine receptors (DHPRs) in the membrane: 'normal' and 'silent' DHPRs. The normal DHPRs behave like classical L-type channels and have the 'normal' voltage dependence. The other population, which is about 2–3 times larger, has a voltage dependence that is shifted to the left by about 10 mV, but remains silent during depolarizations, because it is coupled to an unknown intracellular protein. For the sake of argument, we will refer to the blocking protein as the RyR, because it is an attractive candidate and because both ryanodine and caffeine inhibit tail currents and facilitation (Fig. 7). It is possible, however, that the relevant molecule might be a linking protein such as triadin or the FK 506 binding protein or some other protein or molecule related to E–C coupling (Flucher, Andrews, Fleischer, Marks, Caswell & Powell, 1993; Timerman, Ogunbumni, Freund, Wiederrecht, Marks & Fleischer, 1993).

In the resting state, the RyR is tightly coupled to the silent DHPRs (possibly involving an unidentified link protein). Upon depolarization, the silent DHPRs function as voltage sensors and induce depolarization-induced Ca^{2+} release

(DICR) through the interaction with the RyR. The kinetics of opening of the silent DHPRs is comparable with that of the normal DHPRs (τ , \sim 30 ms; see Fig. 6), but the tight coupling prevents current flow through the DHPRs (high-affinity block). However, the longer and stronger the depolarization, the more and faster RyRs inactivate. This inactivation constitutes a conformational change such that the tight coupling of the RyR to the DHPR changes towards a very unstable conformation (low-affinity block). This conformation can be easily broken by repolarization resulting in conduction of the uncoupled DHPRs, giving rise to the large tail currents. Thus, the slow activation of the tail currents does not reflect the true activation kinetics of the 'silent' DHPRs nor does the strong depolarization needed to activate the tail currents reflect the true voltage dependence of the 'silent' DHPRs. Both are just the conditions required to dissociate them from the RyR and to make them visible.

With respect to the effects of repolarization the data also suggest the following. (1) For the previously silent Ca^{2+} channels to conduct, the repolarization has to be strong enough to overcome the proposed low-affinity block and unplug the channel pore. According to our data this requires repolarizations to +10 mV or below, which may also be the reason for the lack of facilitation at potentials above this (see Fig. 1). (2) At more negative repolarizations, the Ca^{2+} channels will deactivate (deactivation rates accelerate with hyperpolarization). (3) The RyR will reassociate with the DHPR to return to the tight coupling conformation (again, reassociation rates accelerate with hyperpolarization). However, reassociation proceeds at a slower rate than the deactivation time constant of DHPRs, thus determining the time window for 'unplugged' DHPRs to produce facilitation.

Indeed, the kinetic analysis of the reversal of facilitation revealed two distinct phases. The very fast reversal of facilitation (τ_{rev1} in Fig. 5C) may not be strictly regarded as a facilitated state of the Ca^{2+} channels. It probably reflects the degree of deactivation of both normal and anomalous Ca^{2+} channels. If the test pulse is delivered before a substantial fraction of Ca^{2+} channels have deactivated,

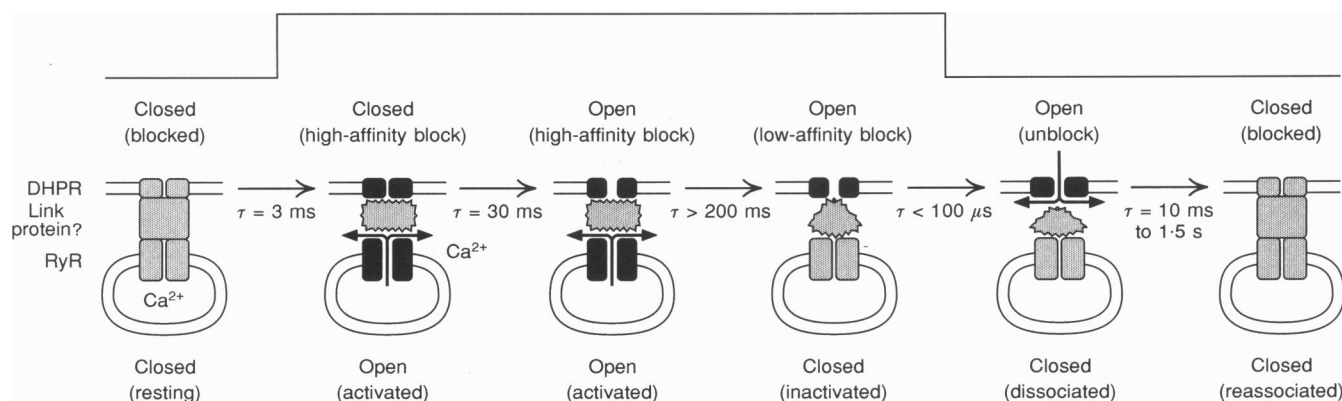


Figure 8. Model

See text for discussion. DHPR, dihydropyridine receptor; RyR, ryanodine receptor.

facilitation will be stronger, simply because the channels remain activated. However, longer repolarizations will quickly decrease the amount of facilitation, as deactivated channels need to be reactivated in order to be able to contribute to facilitation (cf. the traces in Fig. 5A obtained at 0.5 and 32 ms repolarizations to -40 mV).

On the other hand, the slower phase of the reversal of facilitation (τ_{rev2}) can be considered as a truly facilitated state, since it occurs even when channels are allowed to completely deactivate (Fig. 5C). Deactivated Ca²⁺ channels are still available for reactivation. In fact, this is the basis for facilitation, since the total Ca²⁺ current of the facilitated test pulse receives contributions from the 'normal' and untethered 'silent' Ca²⁺ channels (both components can be separated by the subtraction of the control current from the total current, see Fig. 6). However, the facilitated current does not behave in an identical manner to the control current. The net facilitated current decays with a time constant of about 1.5 s at 0 mV (Fig. 6). This apparent inactivation might be due to the reassociation of RyRs with the DHPRs, which replugs open channels and returns them to the silent state again. Thus, we would like to suggest that the reversal of facilitation reflects the voltage-dependent reassociation of the blocking particle with the anomalous Ca²⁺ channels.

In summary, our data support the concept of silent Ca²⁺ channels in skeletal muscle myoballs. These channels are recruited during strong and long-lasting depolarizations but also require repolarization to produce excessive tail currents. The tail currents may reflect an unblock from a blocking particle that remains unidentified at the molecular level but appears to be related to the RyR or some other protein involved in E-C coupling. Unblocked Ca²⁺ channels can be reactivated and contribute to Ca²⁺ influx during a subsequent depolarization, thus forming the basis of facilitation.

- ARTALEJO, C. R., DAHMER, M. K., PERLMAN, R. L. & FOX, A. P. (1991). Facilitation of Ca²⁺ current in bovine chromaffin cells is due to recruitment of a second type of whole-cell current with novel properties. *Journal of Physiology* **432**, 681–707.
- ARTALEJO, C. R., ROSSIE, S., PERLMAN, R. L. & FOX, A. P. (1992). Voltage-dependent phosphorylation may recruit Ca²⁺ current facilitation in chromaffin cells. *Nature* **358**, 63–66.
- BEAN, B. P. (1989). Neurotransmitter inhibition of neuronal calcium channel currents by changes in channel voltage dependence. *Nature* **340**, 153–156.
- DOLPHIN, A. C. (1990). G protein modulation of calcium currents in neurons. *Annual Review of Physiology* **52**, 243–255.
- ELMSLIE, K. S., ZHOU, W. & JONES, S. W. (1990). LHRH and GTP γ S modify calcium current activation in bullfrog sympathetic neurons. *Neuron* **5**, 75–80.
- FELDMAYER, D., MELZER, W., POHL, B. & ZÖLLNER, P. (1990). Fast gating kinetics of the slow Ca²⁺ current in cut skeletal muscle fibres of the frog. *Journal of Physiology* **425**, 347–367.
- FELDMAYER, D., MELZER, W., POHL, B. & ZÖLLNER, P. (1992). Modulation of calcium current gating in frog skeletal muscle by conditioning depolarization. *Journal of Physiology* **457**, 639–653.
- FENWICK, E. M., MARTY, A. & NEHER, E. (1982). Sodium and calcium channels in bovine chromaffin cells. *Journal of Physiology* **331**, 599–635.
- FLEIG, A. & PENNER, R. (1995). Excessive repolarization-dependent calcium currents induced by strong depolarizations in rat skeletal myoballs. *Journal of Physiology* **489**, 41–53.
- FLUCHER, B. E., ANDREWS, S. B., FLEISCHER, S., MARKS, A. R., CASWELL, A. & POWELL, J. A. (1993). Triad formation: organization and function of the sarcoplasmic reticulum calcium release channel and triadin in normal and dysgenic muscle in vitro. *Journal of Cell Biology* **123**, 1161–1174.
- HOSHI, T., ROTHLEIN, J. & SMITH, S. J. (1984). Facilitation of Ca²⁺-channel currents in bovine adrenal chromaffin cells. *Proceedings of the National Academy of Sciences of the USA* **81**, 5871–5875.
- IKEDA, S. R. (1991). Double-pulse calcium channel current facilitation in adult rat sympathetic neurones. *Journal of Physiology* **439**, 181–214.
- JOHNSON, B. D., SCHEUER, T. & CATTERALL, W. A. (1994). Voltage-dependent potentiation of L-type Ca²⁺ channels in skeletal muscle cells requires anchored cAMP-dependent protein kinase. *Proceedings of the National Academy of Sciences of the USA* **91**, 11492–11496.
- PELZER, D., PELZER, S. & McDONALD, T. F. (1990). Properties and regulation of calcium channels in muscle cells. *Reviews of Physiology, Biochemistry and Pharmacology* **114**, 107–207.
- PIETROBON, D. & HESS, P. (1990). Novel mechanism of voltage-dependent gating in L-type calcium channels. *Nature* **346**, 651–655.
- PORZIG, H. (1990). Pharmacological modulation of voltage-dependent calcium channels in intact cells. *Reviews of Physiology, Biochemistry and Pharmacology* **114**, 209–262.
- SCOTT, R. H. & DOLPHIN, A. C. (1987). Activation of a G protein promotes agonist response to calcium channel ligands. *Nature* **330**, 760–762.
- SCULPTOREANU, A., SCHEUER, T. & CATTERALL, W. A. (1993). Voltage-dependent potentiation of L-type Ca²⁺ channels due to phosphorylation by cAMP-dependent protein kinase. *Nature* **364**, 240–243.
- TIMERMAN, A. P., OGUNBUMNI, E., FREUND, E., WIEDERRECHT, G., MARKS, A. R. & FLEISCHER, S. (1993). The calcium release channel of sarcoplasmic reticulum is modulated by FK-506-binding protein. *Journal of Biological Chemistry* **268**, 22992–22999.
- TRAUTWEIN, W. & HESCHELER, J. (1990). Regulation of cardiac L-type calcium current by phosphorylation and G proteins. *Annual Review of Physiology* **52**, 257–274.

Acknowledgements

We thank Erwin Neher for critical discussions and comments on the manuscript and Michael Pilot for excellent technical assistance. We acknowledge support by the following institutions: Deutsche Forschungsgemeinschaft, Sonder-forschungsbereich 236, Hermann-und Lilly-Schilling-Stiftung.

Author's email address

A. Fleig: afleig@gwdg.de

Received 19 October 1995; accepted 28 February 1996.